Published in final edited form as:
Cell Stem Cell. 2009 December 4; 5(6): 624–633. doi:10.1016/j.stem.2009.10.003.

Imbalance between GABAergic and Glutamatergic Transmission Impairs Adult Neurogenesis in an Animal Model of Alzheimer's Disease

Binggui Sun[1,2,3], **Brian Halabisky**[1,2,3], **Yungui Zhou**[1], **Jorge J. Palop**[1,2], **Guiqiu Yu**[1], **Lennart Mucke**[1,2], and **Li Gan**[*,1,2]

[1]Gladstone Institute of Neurological Disease, University of California, San Francisco, California 94158, USA

[2]Department of Neurology, University of California, San Francisco, California 94158, USA

SUMMARY

Adult neurogenesis regulates plasticity and function in the hippocampus, which is critical for memory and vulnerable to Alzheimer's disease (AD). Promoting neurogenesis may improve hippocampal function in AD brains. However, how amyloid β (Aβ), the key AD pathogen, affects the development and function of adult-born neurons remains unknown. Adult-born granule cells (GCs) in human amyloid precursor protein (hAPP) transgenic mice, an AD model, showed greater dendritic length, spine density, and functional responses than controls early in development, but were impaired morphologically and functionally during later maturation. Early inhibition of $GABA_A$ receptors to suppress GABAergic signaling or late inhibition of calcineurin to enhance glutamatergic signaling normalized the development of adult-born GCs in hAPP mice with high Aβ levels. Aβ-induced increases in GABAergic neurotransmission or an imbalance between GABAergic and glutamatergic neurotransmission may contribute to impaired neurogenesis in AD.

INTRODUCTION

Alzheimer's disease (AD), the most common neurodegenerative disorder, results in severe neuronal and synaptic loss in several brain regions important for learning and memory (Scheff and Price, 2003). One of the most affected regions is the hippocampal formation, which includes the dentate gyrus (DG), where neurogenesis persists through adulthood in rodents and humans (Altman and Das, 1965; Eriksson et al., 1998). In the DG, adult-born granule cells (GCs) may contribute to cognition and mood regulation (Clelland et al., 2009; Duan et al., 2007; Santarelli et al., 2003; Shors et al., 2001). Ablation of neurogenesis impairs some aspects of learning and memory (Imayoshi et al., 2008; Saxe et al., 2006; Snyder et al., 2005b). During a critical period of time (1–1.5 months of cell age), adult-born GCs exhibit enhanced long-term potentiation with increased potentiation amplitude and decreased induction threshold,

[*]**Correspondence** Li Gan, PhD, Gladstone Institute of Neurological Disease, 1650 Owens Street, San Francisco, CA 94158, (415) 734-2425, lgan@gladstone.ucsf.edu.

[3]Authors contributed equally

suggesting possible roles in experience-induced plasticity (Ge et al., 2007; Schmidt-Hieber et al., 2004).

Although increased levels of pathogenic amyloid-β (Aβ) assemblies likely contribute causally to AD (Tanzi and Bertram, 2005), there is much debate about if and how Aβ affects adult neurogenesis in the hippocampus. Some studies found that neurogenesis is increased in AD brains (Jin et al., 2004b), but others did not (Boekhoorn et al., 2006; Li et al., 2008). Conflicting results also came from studies using BrdU labeling and neuronal or glial markers in different lines of transgenic mice expressing human amyloid precursor protein (hAPP) (Donovan et al., 2006; Haughey et al., 2002; Lopez-Toledano and Shelanski, 2007; Verret et al., 2007). Notably, most of these studies focused on the number rather than the function of adult-born GCs. We set out to investigate morphological and functional development of adult-born GCs in hAPP mice with high or low levels of Aβ.

Adult hippocampal neurogenesis is tightly regulated by neuronal activity, particularly by the balance between GABAergic and glutamatergic inputs (Zhao et al., 2008). At early stages of cell development, tonic activation of $GABA_A$ receptors by ambient GABA regulates neuronal differentiation of hippocampal progenitor cells (Tozuka et al., 2005) and dendritic growth of newborn GCs in the adult brain (Ge et al., 2008). Later, stimulation of glutamate receptors becomes critical in shaping the plasticity of adult-born GCs (Tashiro et al., 2006a). Because Aβ-induced neurological deficits are closely associated with aberrant excitatory and inhibitory activity (Palop et al., 2007), we hypothesized that Aβ affects adult neurogenesis by altering the balance between excitatory and inhibitory inputs onto adult-born GCs.

To test this hypothesis, adult-born GCs were labeled with a retroviral vector that encodes enhanced green fluorescent protein (EGFP) and allows for birth-dating and tracking of adult-born GCs (van Praag et al., 2002; Zhao et al., 2006). The effects of high Aβ levels on the morphological and functional development of adult-born GCs were assessed in hAPP transgenic mice from line J20 (hAPP-J20), which express hAPP with familial AD (FAD) mutations (Mucke et al., 2000), by confocal microscopy and patch-clamp recordings. We also used drug treatments to determine if shifting the balance between GABAergic and glutamatergic signaling during key developmental stages improves adult neurogenesis with high Aβ levels.

RESULTS

Accelerated Early Development of Adult-Born GCs in hAPP-J20 Mice

To assess the effects of hAPP/Aβ on the morphological and functional development of adult-born GCs, adult-born GCs of hAPP-J20 mice and nontransgenic (NTG) controls were labeled with an EGFP-expressing retroviral vector (CAG-EGFP) (Zhao et al., 2006), which was stereotaxically injected into the DG. Because the virus labels only dividing cells, the day of the injection marked the ‘birth date’ of neurons, which were identified by EGFP and NeuN immunostaining (Figure 1A). Neurons were readily discriminated from dividing astrocytes or oligodendrocytes by their morphology and the NeuN marker. To follow critical developmental stages of adult-born GCs, we analyzed labeled neurons at 14, 18, 21, 25, 28, 56, and 122 days post infection (dpi). Unless indicated otherwise, we examined adult-born GCs in 2–3-month-old NTG and age-matched hAPP-J20 mice, which have not yet formed amyloid plaques but already exhibit neuronal and behavioral deficits that are likely caused by soluble Aβ oligomers (Cheng et al., 2007) .

We first determined if the $GABA_A$ Cl^- current reversal potentials (E_{GABA}s) of adult-born GCs in hAPP-J20 mice differ from those in NTG mice. Normally, E_{GABA} transitions from depolarizing to hyperpolarizing during the third week after the birth of GCs (Ge et al., 2006;

Zhao et al., 2006). To compare the E_{GABA} of adult-born GCs in hAPP-J20 and NTG mice, we used gramicidin-perforated patch-clamp to record evoked $GABA_A$ receptor–mediated Cl^- currents at membrane potentials of –80 to –20 mV. The E_{GABA}s of adult-born GCs were significantly more hyperpolarized in hAPP-J20 mice than in NTG mice at 14, 18, and 21 dpi, while their resting membrane potentials (RMPs) remained at ~ −60 mV throughout all developmental stages (Figure 1B). Thus, consistent with previous findings (Ge et al., 2006; Zhao et al., 2006), the E_{GABA}s of adult-born GCs in NTG mice were more depolarizing than RMP at both 14- and 18- dpi. In contrast, the E_{GABA} of adult-born GCs in hAPP-J20 mice was not depolarized at 14 dpi and became more hyperpolarizing than RMP from 18 dpi on. These results suggest that adult-born GCs exhibit a much faster developmental transition in hAPP-J20 mice than in NTG mice during the first 2 to 3 weeks after their birth. By 28 dpi, the E_{GABA}s of adult-born GCs in both NTG and hAPP-J20 mice were similarly hyperpolarized. No difference was observed in RMP or E_{GABA} of prenatally born (mature) GCs in NTG and hAPP-J20 mice.

Morphological analyses revealed that the dendrites of adult-born GCs were longer in hAPP-J20 than NTG mice at 18 dpi, and the spine density of 18-day-old GCs in hAPP-J20 mice was twice that in NTG mice (Figures 1E, F). Functionally, adult-born GCs exhibited stronger evoked inhibitory post-synaptic currents (eIPSCs) and excitatory post-synaptic currents (eEPSCs) in hAPP-J20 mice than NTG controls in the first 2–3 weeks, especially at 21 dpi (Figures 1G–J). Thus, adult-born GCs in hAPP-J20 mice undergo accelerated morphological and functional development during the first 3 weeks after their birth.

Adult-Born GCs in hAPP-J20 Mice Display Impaired Maturation and Functional Responses

The dendritic growth of wild type adult-born GCs starts to plateau at about 28 days after their birth (Zhao et al., 2006). Despite evidence of accelerated growth in the first 3 weeks, the dendrites of 28-day-old adult-born GCs were shorter and had fewer branches in hAPP-J20 mice than NTG mice (Figures 2A–C). In addition, the dendritic spine density of 28-day-old adult-born GCs was lower in hAPP-J20 mice than NTG mice (Figures 2D, E). The impaired dendritic morphogenesis persisted to 56 and 122 dpi, when adult-born GCs are considered indistinguishable from preexisting GCs in the DG (Zhao et al., 2006). Dendrites of 56- or 122-day-old adult-born GCs were still shorter with fewer dendritic branches and spines in hAPP-J20 mice than in NTG mice (Figures 2B, E).

In whole-cell patch-clamp recordings, we examined how well 28-day-old adult-born GCs respond to synaptic inputs. Consistent with the impaired dendritic morphogenesis, eIPSCs in 28-day-old adult-born GCs were much smaller in hAPP-J20 than in NTG mice (Figures 2F, G). These results were in sharp contrast to the elevated levels of eIPSCs in 21-day-old adult-born GCs in hAPP-J20 mice (Figure 1H). In hAPP-J20 mice, eIPSCs decreased from 21 to 25 dpi (205.9 pA ± 54.8 to 145.8 pA ± 35.8) and further at 28 dpi (Figures 2F, G). To dissect the mechanism underlying the biphasic developmental changes, we measured the amplitudes of mIPSCs of adult-born GCs at 18, 21, 25, and 28 dpi. In NTG mice, amplitudes of mIPSCs of adult-born GCs increased from 18 to 28 dpi, suggesting gradual maturation. In contrast, amplitudes of mIPSCs declined from 18 to 28 dpi in hAPP-J20 mice, especially from 21–28 dpi (Figure 2H). These results suggest that the decrease of eIPSCs during this period in hAPP-J20 mice likely reflects, at least in part, a reduction in the number/function of post-synaptic receptors on adult-born GCs.

Mouse Age, but Not Wildtype hAPP, Affects Adult-Born GC Development

To determine if these alterations are caused by hAPP itself or Aβ, we analyzed adult-born GCs in 2–3-month-old hAPP-I5 mice. hAPP-I5 mice express wildtype hAPP at levels comparable to those of FAD-mutant hAPP in hAPP-J20 mice, but have much lower levels of Aβ (Mucke

et al., 2000). At 28 dpi, adult-born GCs in hAPP-I5 mice exhibited no significant abnormalities in dendritic length, branching points, and spine density (Figures 3A–C). These results support the notion that the impaired dendritic morphogenesis of adult-born GCs in hAPP-J20 mice is caused by high levels of soluble Aβ rather than hAPP, although other effects of the FAD mutations in hAPP-J20 mice cannot be excluded.

To assess the effects of mouse age on the alterations of adult-born GC development, we next compared adult-born GCs in 3–4-week-old hAPP-J20 and NTG mice. At 28 dpi, the dendritic lengths of adult-born GCs were shorter in hAPP-J20 mice than in NTG mice, but their spine densities were similar (Figures 3D, E). When adult-born GCs were labeled in mice that were 2–3 months or 6–7 months of age, 28-day-old adult-born GCs in hAPPJ20 mice had both shorter dendrites and lower spine densities than GCs in NTG controls (Figures 3F–I). Moreover, 28-day-old GCs born in 6–7-month-old hAPP-J20 mice had fewer spines than those born in 2–3-month-old ($P < 0.01$, one way ANOVA) or 3–4-week-old ($P < 0.001$, one way ANOVA) hAPP-J20 mice. Therefore, as hAPP-J20 mice age, the morphological impairments seen at 28 dpi become progressively worse. Since Aβ, especially Aβ42, accumulates with age, we compared Aβ levels in hAPP-J20 mice at 3–4-weeks and 2–3-months of age. Levels of Aβ42 and ratios of Aβ42/Aβ1-x were higher in hippocampus of 2–3-month-old hAPP-J20 mice than in 3–4-week-old hAPP-J20 mice (Figure S1). Thus, the age-dependent worsening of dendritic morphology of adult-born GCs could be related to an increase in the levels of Aβ42, which is more neurotoxic than Aβ40 (McGowan et al., 2005).

Inhibitory Synaptic Transmission Is Favored in Adult-Born GCs of hAPP-J20 Mice

Aβ elicits aberrant excitatory neuronal activity that is associated with remodeling of inhibitory circuits and an increased number of inhibitory synaptic contacts onto GCs in the DG (Palop et al., 2007). Compared with NTG mice, hAPP-J20 mice showed aberrant sprouting of neuropeptide Y (NPY)/GABAergic axonal terminals in the molecular layer of the DG (Figure 4A). These inhibitory terminals make synaptic contacts onto the dendrites of GCs (Freund and Buzsaki, 1996). We characterized the frequencies of mIPSCs onto adult-born GCs at 18, 21, 25, and 28 dpi in NTG and hAPP-J20 mice. From 18–25 dpi, the frequency of mIPSCs of adult-born GCs was markedly higher in hAPP-J20 mice than in NTG mice (Figures 4B, C), suggesting an increase in the number of effective inhibitory synaptic contacts onto adult-born GCs in hAPP-J20 mice. The lack of increase at 28 dpi could be related to the reduction in the number of effective post-synaptic sites (Figure 2H).

Because adult hippocampal neurogenesis is tightly regulated by the balance between GABAergic and glutamatergic inputs (Zhao et al., 2008), we next measured the frequency of mEPSCs of adult-born GCs. In contrast to those of mIPSCs, the frequency of mEPSCs was similar in hAPP-J20 and NTG mice (Figures 4D, E). As a result, the ratio of mIPSC/mEPSC frequency in 18- and 21-day-old adult-born GCs was higher in hAPP-J20 mice than in NTG mice (Figure 4F). The ratio of mIPSC/mEPSC peak amplitude in 18- and 21-day-old adult-born GCs was also higher in hAPP-J20 mice than NTG mice (Figure S2), consistent with excessive GABAergic inputs in hAPP-J20 mice. We next measured spontaneous inhibitory and excitatory synaptic currents (sIPSCs and sEPSCs) of 18-, 21-, 25-, and 28-day-old GCs by leaving the endogenous pre-synaptic activities unblocked (–TTX). The ratios of sIPSC/sEPSC frequency (Figure 4G) and peak amplitude (Figure S2) of adult-born GCs were both higher in hAPP-J20 mice than NTG mice at 18, 21, and 25 dpi, further supporting an imbalance of GABAergic and glutamatergic inputs onto adult-born GCs in hAPP-J20 mice.

Inhibition of $GABA_A$ Receptors Ameliorates Developmental Alterations of Adult-Born GCs in hAPP-J20 Mice

We hypothesize that the accelerated early development of adult-born GCs in hAPP-J20 mice might result from excessive GABAergic inputs. To test this hypothesis, we injected the $GABA_A$ receptor antagonist picrotoxin (PTX) into mice intraperitoneally to counteract GABAergic signaling for the first 7 days after viral infection of adult-born GCs. A low dose (1 mg/kg) was used so that no convulsive seizure activity was observed in either NTG or hAPP-J20 mice. Early PTX treatments (1–7 dpi) reduced the excessive spine growth of 18-day-old adult-born GCs in hAPP-J20 mice (Figures 5A, B), but failed to reduce their increased dendritic length (Figures 5C, D). Early PTX treatments also increased the abnormally low spine density and dendritic length in 28-day-old adult-born GCs of hAPP-J20 mice (Figures 5B, D), suggesting that excessive GABAergic inputs at early developmental stages prevented normal dendritic maturation of adult-born GCs in hAPP-J20 mice. Notably, early inhibition of $GABA_A$ receptors decreased spine density and dendritic length of 28-day-old adult-born GCs in NTG mice (Figures 5B, D). These results indicate that, while excessive amounts of GABAergic signaling in hAPP mice is detrimental, GABAergic signaling at early stage is required for normal dendritic maturation (Ge et al., 2006).

In contrast to the robust effects of early inhibition of $GABA_A$ receptors (1–7 dpi), late inhibition (14–27 dpi) did not exert significant effects on either spine density or dendritic length of 28-day-old GCs in NTG mice, suggesting a minor role of GABAergic signaling in the late-stage maturation of adult-born GCs (Figures 5E, F). In agreement with this notion, blockade of GABAergic signaling from 14–27 dpi failed to restore dendritic length and increased spine density only modestly in hAPP-J20 mice (Figures 5E, F).

Inhibiting Calcineurin Improves Dendritic Morphogenesis of Adult-Born GCs in hAPP-J20 Mice

Besides GABAergic input, glutamatergic signaling also regulates the development of adult-born GCs (Zhao et al., 2008). Glutamatergic signaling is particularly critical for the survival of adult-born GCs and their integration into functional neural circuits during the third and fourth week after their birth (Tashiro et al., 2006a). In dissociated hippocampal neurons or organotypic hippocampal slice cultures, Aβ reduces glutamatergic neurotransmission by enhancing the endocytosis of NMDA- and AMPA-type glutamate receptors, which requires the activation of calcineurin (Hsieh et al., 2006; Shankar et al., 2007; Snyder et al., 2005a). Notably, cerebral calcineurin activity was signficantly higher in 5-month-old hAPP mice from line Tg2576 than in age-matched NTG controls (Dineley et al., 2007). To counteract Aβ-induced depression of glutamatergic neurotransmission, we therefore treated hAPP-J20 mice with an inhibitor of calcineurin, FK-506, from 14 to 27 dpi. This treatment period coincides with the formation of excitatory synapses. At 5 mg/kg, but not 2 mg/kg (data not shown), FK-506 completely restored dendrite length and spine density of 28-day-old adult-born GCs in hAPP-J20 mice, but had no effects on those in NTG mice (Figure 6A–C). These results suggest that calcineurin activation, which reduces glutamatergic neurotransmission, is involved in Aβ-induced maturation deficits of adult-born GCs in hAPP-J20 mice.

DISCUSSION

Our study demonstrates that increased levels of Aβ elicit complex changes in the development and maturation of adult-born GCs, resulting in accelerated morphological and functional development at early stages and in morphological and functional deficits at later stages of maturation. We further provide electrophysiological and pharmacological evidence for an Aβ-dependent imbalance between GABAergic and glutamatergic inputs to adult-born GCs and

demonstrate that suppressing GABAergic signaling or enhancing glutamatergic signaling normalizes the development of adult-born GCs even in the presence of high Aβ levels.

Because adult-born GCs matured normally in hAPP-I5 mice with high hAPP levels but relatively low Aβ levels (Mucke et al., 2000), the abnormalities in neurogenesis in hAPP-J20 mice were unlikely from hAPP itself, but from high Aβ levels or another consequence of the FAD mutations expressed in this line. Because adult-born GCs showed severe abnormalities in 2–3-month-old hAPP-J20 mice that had not yet formed amyloid plaques, the abnormalities in neurogenesis do not depend on Aβ deposition and are more likely caused by soluble nonfibrillar Aβ assemblies. Abnormalities of adult-born GCs were more prominent in older hAPP-J20 mice than in younger hAPP-J20 mice. This difference probably reflects age- or time-dependent increases in pathogenic Aβ42 assemblies. Aging-related changes in cofactors that affect neuronal susceptibility to Aβ may also play a role.

We found that Aβ affects the morphological and functional growth of adult-born GCs differently at different stages of cellular development. During the first 3 weeks, Aβ accelerated the development of adult-born GCs, but induced morphological and functional deficits of adult-born GCs when they were 28 days or older. The marked decline of the peak amplitude of eIPSCs from 21 to 28 dpi could result from a reduced number of inhibitory synaptic contacts or reductions in the effectiveness of the post-synaptic response to pre-synaptic transmitter release. Since the peak amplitudes of mIPSCs markedly declined from 21 to 28 dpi, the decrease in eIPSC peak amplitudes during this period might result largely from postsynaptic mechanisms, most likely a decline in the number of postsynaptic $GABA_A$ receptors. The slight reduction in the mIPSC frequency in adult-born GCs of hAPP-J20 mice from 21 to 28 dpi indicates a minor role for a reduction in the number of inhibitory synaptic contacts.

Earlier studies showed that the number of immature neural progenitor cells expressing doublecortin and Neuro-D was increased in other hAPP transgenic lines (Gan et al., 2008; Jin et al., 2004a) and in AD (Jin et al., 2004b). In contrast, the long-term survival of neuronal progenitor cells was decreased in several hAPP transgenic lines and in AD brains (Boekhoorn et al., 2006; Donovan et al., 2006; Haughey et al., 2002; Li et al., 2008; Verret et al., 2007). Incorporation of BrdU was used to estimate the number of dividing cells in these previous studies. Here we used CAG-GFP retrovirus to label a portion of the dividing cell population in hAPP-J20 and NTG mice. To ensure that we could use GFP^+ GCs labeled with retrovirus to estimate the surviving adult-born GCs, we compared the viral infection efficiency in hAPP-J20 and NTG mice. $GFP^+/BrdU^+$ ratios, measured at 10 dpi, did not differ in NTG and hAPP-J20 mice (Figure S3), suggesting similar infection efficiencies. We observed more retroviral-labeled GFP^+ neurons in hAPP-J20 mice than in NTG mice at 18 dpi, but not at 28 dpi (Figure S3), in agreement with other studies reporting increased numbers of immature neural progenitor cells in AD brains and hAPP mice (Gan et al., 2008; Jin et al., 2004a). Since GABAergic inputs to hippocampal progenitor cells promote activity-dependent neuronal differentiation, the increased ambient GABA may be responsible for the increased number of adult-born GCs in hAPP-J20 mice at early developmental stages.

At early developmental stages, activation of $GABA_A$ receptors leads to depolarization of adult-born GCs and to calcium influx, which activates a network of transcription factors that promote the growth of dendrites and spines (Ben-Ari, 2002; Owens and Kriegstein, 2002). Excessive GABAergic stimulation may underlie the increased spine density of young adult-born GCs in hAPP-J20 mice early on. Inhibition of $GABA_A$ receptors by PTX during the first 7 days after birth effectively halted increased spine density in 18-day-old adult-born GCs in hAPP-J20 mice, suggesting that elevated levels of ambient GABA rather than of synaptically released GABA are the likely cause of accelerated early spine growth. In hAPP-J20 mice, one source of increased ambient GABA in hAPP-J20 mice could be the excessive GABAergic sprouting

in the molecular layer of the DG, possibly as a compensatory response to aberrant Aβ-induced excitatory neuronal activity (Palop et al., 2007).

Our data showed that the adult-born GCs in hAPP-J20 mice were impaired morphologically by 28 dpi and that the impairments could be significantly attenuated by early inhibition of $GABA_A$ receptor–mediated signaling. These findings suggest that excessive early GABAergic signaling also contributes to impaired dendritic maturation. The underlying mechanisms remain unclear. Previous findings showed that GABA itself promotes GABAergic responses from depolarization to hyperpolrization (Ganguly et al., 2001), which could prematurely reduce Ca^{2+} influx and blunt dendritic growth. Consistent with this notion, the E_{GABA}s of adult-born GCs in hAPP-J20 mice had accelerated switch to hyperpolarization, likely due to excessive early GABAergic signaling. In NTG mice, early inhibition of $GABA_A$ receptor–mediated signaling significantly decreased the dendritic length and spine density of adult born-GCs, further highlighting the importance of early GABAergic signaling. In contrast, inhibition of GABAergic signaling from 14 to 27 dpi increased spine density of adult-born GCs only modestly in hAPP-J20 mice and had little effects on dendritic morphogenesis in NTG mice. Thus, late-stage GABAergic signaling appears to play only a minor role in the development and maturation of adult-born GCs.

Inhibition of calcineurin activation by FK506 from 14–27 dpi completely restored the dendritic structure of 28-day-old adult-born GCs in hAPP-J20 mice, but had no significant effects on those born in NTG mice. These results suggest that calcineurin activation, which was elevated in hAPP transgenic mice than NTG controls (Dineley et al., 2007), is involved in Aβ-induced impaired dendritic morphogenesis in developing neurons in vivo. Our results also agree with the requirement of calcineurin for Aβ- induced reduction in spines and in NMDA and AMPA receptors observed in cell or tissue cultures (Hsieh et al., 2006; Snyder et al., 2005a). The efficacy of FK506 in preventing Aβ-dependent spine reduction supports a critical role of glutamatergic signaling in late-stage (14–28 dpi) spine development of adult-born GCs. Earlier studies showed that NMDA receptor signaling plays a key role in the survival of adult-born GCs during the third week after their birth (Tashiro et al., 2006a). We found that FK506 treatment of hAPP-J20 mice increased not only spine growth, but also the number of retrovirally labeled adult-born GCs at 28 dpi (Figure S4).

From 18 to 28 days after the birth of adult-born GCs, spine densities increased by 300% (from 0.31 ± 0.06 to 1.27 ± 0.04 per μm) in NTG mice but only by 14% (from 0.68 ± 0.07 to 0.78 ± 0.02 per μm) in hAPP-J20 mice. It remains unclear if spine growth in adult-born GCs of hAPP-J20 mice slows down drastically during this period or if their spine growth is counteracted by an Aβ-induced loss of spines (Hsieh et al., 2006; Shankar et al., 2008). Although GCs in 11-month-old hAPP-J20 mice have a decreased number of spines (Moolman et al., 2004), the spine density did not appear to differ in putatively prenatally born GCs labeled by Lenti-EGFP in 2–3-month-old hAPP-J20 mice and NTG controls (Figure S5). Conceivably, GCs are more vulnerable to the effects of Aβ when born postnatally than when born prenatally. In addition, the levels of pathogenic Aβ42 assemblies may be lower prenatally than postnatally, and the alterations of adult-born GCs may depend on Aβ-induced increases in GABAergic signaling that develop only postnatally. These possibilities are not mutually exclusive.

Our findings implicate impaired neurogenesis in cognitive dysfunction and suggest that restoring neurogenesis might enhance cognition. Although we did not directly address this question here, previous results indicate that treatments of PTX or FK506, which restored the development of adult-born GCs in our studies, also protected against Aβ-associated behavior deficits. For example, treatment with PTX at a non-epileptic dose for 10 days ameliorated memory deficits in adult APP/PS1 mice (Yoshiike et al., 2008) and improved object recognition memory in Ts65Dn mice that carry three copies of APP (Fernandez et al., 2007). Inhibition of

calcineurin by FK506 reversed the intermediate-and long-term recognition memory deficits in Tg2576 mice (Dineley et al., 2007; Taglialatela et al., 2009). However, more studies are needed to establish if the PTX- or FK506-induced cognitive improvements are mechanistically linked to enhancements in adult neurogenesis.

EXPERIMENTAL PROCEDURES

Animals

Heterozygous hAPP transgenic mice from line J20 (hAPP-J20), which produce hAPP with the Swedish (K670N, M671L) and Indiana (V717F) FAD mutations (Mucke et al., 2000), and age-matched NTG littermates were injected with viral vectors when they were 3–4 weeks, 2–3 months, or 6–7 months of age. We also analyzed 2–3-month-old heterozygous hAPP transgenic mice from line I5 (hAPP-I5), which expresses wildtype hAPP at levels comparable to those of mutant hAPP in hAPP-J20 mice (Mucke et al., 2000). All animal studies were approved by the animal care and use committee of the University of California, San Francisco.

ELISA

Aβ levels in the hippocampus of 3–4-week-old and 2–3-month-old hAPP-J20 mice were measured by ELISA as described (Johnson-Wood et al., 1997).

Preparation and Stereotaxic Injection of Viral Vectors

Postnatally born GCs in the hippocampus of adult (2–3-month- and 6–7-month-old) and young (3–4-week-old) mice were labeled by infection with a murine Moloney leukemia virus-based retroviral vector (CAG–EGFP, a gift from Fred Gage, Salk Institute, La Jolla, CA). Concentrated viral solutions were prepared by co-transfection of retroviral vectors and VSV-G (envelope vector) into HEK293T cells, followed by ultracentrifugation of viral supernatant as described (Tashiro et al., 2006b). To label adult-born GCs, viral solution (3 μl) was delivered into the DG by stereotaxic injection (0.5 μl per min). For 2– 3-month-old and 6–7-month-old mice, we used the following coordinates (Paxinos and Franklin, 2001): anterior-posterior, −2.1 mm; lateral, ±1.7 mm; and vertical, −2.0 mm. For 3–4-week-old mice, the distance (*d*) between bregma and lambda in anterior-posterior coordinates was measured to determin the injection positions as follows: anterior-posterior, $-1/2 \times d$ mm; lateral, ±1.7 mm; and vertical, −1.9 mm. For all injections, bregma was the reference point. A lentiviral vector expressing EGFP (FUGW) was injected into the DG to label GCs as described (Mueller-Steiner et al., 2006).

Drug Treatment

Some mice received a daily intraperitoneal (i.p.) injection of PTX (Sigma, 1 mg/kg body weight) or vehicle (PBS) from dpi 1–7 or 14–27, or a daily subcutaneous injection of FK506 (Sigma, 2 or 5 mg/kg body weight) or vehicle (DMSO) from dpi 14–27. For BrdU (5-bromo-2-deoxyuridine) treatment, mice were injected stereotaxically with retrovirus first, and then received an i.p injection of BrdU (Sigma; 50 mg/kg, once per day) starting the next day for 3 days. One week after the last injection of BrdU, mice were perfused with saline and fixed with 4% PFA for immunostaining.

Immunofluorescence

Immunofluorescent staining was described previously (Mueller-Steiner et al., 2006). Briefly, coronal brain sections (30 μm) were blocked with blocking buffer (10% serum, 1% milk, 0.2% gelatin in PBS) and incubated with rabbit anti-GFP (Invitrogen, 1:500), mouse anti-NeuN (Chemicon, 1:1000), rabbit anti-NPY (ImmunoStar, 1:4000), and mouse anti-BrdU (Roche, 1:200), followed by incubation with appropriate secondary antibodies conjugated with FITC or Texas Red (Vector Laboratories, 1:150). All images of dendritic structures were obtained

from CAG-EGFP injected brains stained with anti-GFP antibody to amplify the GFP signal. For BrdU staining, sections were pretreated with 2 N HCl at 37°C for 30 min, washed in 100 mM borate buffer (pH 8.5) for 10 min, and then in TBST-Triton (10 mM Tris-HCl, pH 7.4, including 150 mM NaCl, 0.05% Tween-20, and 0.1% Triton X-100) for 30 min at room temperature before incubation with blocking buffer.

Confocal Image Analysis

For dendritic analysis, z-series stacks of optical images were obtained at 1-μm intervals with a 40× objective on a confocal microscope (Radiance 2000, Bio-Rad, Hercules, CA). Two-dimensional projections of each z-series were created using Adobe Photoshop CS. All individual GFP-positive GCs that had continuous dendritic trees were analyzed for total dendritic length and branch numbers. The total dendritic length of all individual GFP-positive GCs was measured using Image J, and their branches were counted manually from the same images. For spine analysis, z-series stacks of confocal images of GFP-labeled dendritic segments in the molecular layer were obtained at 0.5-μm intervals using a confocal microscope, a 60× oil lens and a digital zoom of 4.0. Projections of z-series were created with Adobe Photoshop CS. The length of each dendritic segment was measured by tracing the center of the dendritic shaft with Image J. The number of spines was counted manually. The spine density was calculated by dividing the total number of spines by the length of the dendritic segment.

Acute Slice Preparation

NTG and hAPP-J20 mice (2–3-month-old) were anesthetized with Avertin (tribromoethanol, 250 mg/kg) and decapitated 14, 18, 21, 25, or 28 days after the injection of CAG-GFP. Slicing was done under conditions favorable for adult mice (Aghajanian and Rasmussen, 1989). Briefly, brains were quickly removed and placed in ice-cold solution containing (in mM) 2.5 KCl, 1.25 $NaPO_4$, 10 $MgSO_4$, 0.5 $CaCl_2$, 26 $NaHCO_3$, 11 glucose, and 234 sucrose (pH ~7.4; 305 mOsmol). 350-μm horizontal slices were cut using a vibratome and collected in the above solution. Slices were then incubated for 30 min in standard artificial cerebrospinal fluid (ACSF; 30°C) containing (in mM): 2.5 KCl, 126 NaCl, 10 glucose, 1.25 NaH_2PO_4, 1 $MgSO_4$, 2 $CaCl_2$, and 26 $NaHCO_3$ (290 mOsmol; gassed with 95% O_2–5% CO_2, pH ~7.4). Subsequently, slices were maintained at room temperature for ≥ 30 min before recording. No recordings were made on slices > 5 hours after dissection. Individual slices were transferred to a submerged recording chamber where they were maintained at 30°C and perfused with ACSF at a rate of 2 ml/min.

Electrophysiological Recordings

EGFP-expressing GCs were identified under epifluorescence. Voltage- and current-clamp recordings were obtained using infrared differential interference contrast (IR-DIC) video microscopy. Except as noted, recordings were done in whole cell patch-clamp configuration, in which the intracellular patch pipette solution contained (in mM) 120 Cs-gluconate, 10 HEPES, 0.1 EGTA, 15 $CsCl_2$, 4 $MgCl_2$, 4 Mg-ATP, and 0.3 Na_2-GTP, pH 7.25 adjusted using 1 M CsOH (285–290 mOsm; patch electrode resistance: 3–6 MΩ).

RMP and $GABA_A$ reversal potentials were determined using a perforated patch-clamp configuration, in which the intracellular patch pipette solution contained (in mM) 130 KCl, 5 EGTA, 0.5 $CaCl_2.2H_2O$, 2 $MgCl_2$, and 10 HEPES, pH 7.3, adjusted with 1 M KOH (285–290 mOsm). Gramicidin at a final concentration of 25–50 μg/ml was added to the pipette solution before each experiment. EGFP-labeled GCs were selected at random for electrophysiological recording. To determine the reversal potential of $GABA_A$ receptor-mediated currents, brief pressure pulses (“puffs”; 12–15 ms, 200–275 kPa) of muscimol (100 μM) were applied to the soma of the recorded neuron through a patch pipette. E_{GABA} was determined by where the polarity of the muscimol evoked currents reversed relative to the holding current.

Inhibitory and excitatory synaptic currents in GCs were evoked using a bipolar tungsten electrode (FHC, Bowdoin, ME) placed in the outer molecular layer. Input (stimulus)-output (post-synaptic current [PSC]; I-O) relationships for evoked excitatory and inhibitory PSCs were obtained for each cell. Miniature PSCs were isolated by focally applying TTX (1 μM) to the DG through a local perfusion system (AutoMate Scientific, San Francisco, CA). Miniature PSCs were analyzed by event detection software (wDetecta; Dr. John Huguenard, Stanford University). More detailed descriptions can be found in the Supplementary Methods section.

Statistical Analysis

Statistical analyses were conducted with Graphpad Prism (San Diego, CA) or SPSS (Chicago, IL). Differences among multiple means with one variable (hAPP genotype) were evaluated by one-way ANOVA and Tukey-Kramer post hoc test. Differences among multiple means with two variables (genotype and treatments) were evaluated by two-way ANOVA and Bonferroni multiple comparison posthoc test. Differences between two means were assessed with unpaired, two-tailed t test. Differences between two cumulative histograms were assessed using the two-sample Kolmogorov-Smirnov test. Differences between multiple cumulative histograms were assessed using Kruskal-Wallis one-way analysis of variance. Only values that had $P < 0.05$ were accepted as significant.

Supplementary Material

Refer to Web version on PubMed Central for supplementary material.

Acknowledgments

We thank Chunmei Zhao, Xinyu Zhao and Fred Gage for the CAG-EGFP retroviral vector, Sarah Mueller-Steiner for viral preparations, Robert W. Mahley and Anatol Kreitzer for insightful discussions, Xin Wang for excellent technical support, Stephen Ordway and Gary Howard for editorial review, and Kelley Nelson for administrative assistance. This work was supported in part by a grant from Whittier Foundation (to L.G.), NIH grants AG022074 and NS041787 (to L.M.) and NIH/NCRR CO6 RRO18928 (a facility grant to the J. David Gladstone Institutes).

REFERENCES

Aghajanian GK, Rasmussen K. Intracellular studies in the facial nucleus illustrating a simple new method for obtaining viable motoneurons in adult rat brain slices. Synapse 1989;3:331–338. [PubMed: 2740992]

Altman J, Das GD. Autoradiographic and histological evidence of postnatal hippocampal neurogenesis in rats. J Comp Neurol 1965;124:319–335. [PubMed: 5861717]

Ben-Ari Y. Excitatory actions of gaba during development: the nature of the nurture. Nat Rev Neurosci 2002;3:728–739. [PubMed: 12209121]

Boekhoorn K, Joels M, Lucassen PJ. Increased proliferation reflects glial and vascular-associated changes, but not neurogenesis in the presenile Alzheimer hippocampus. Neurobiol Dis 2006;24:1–14. [PubMed: 16814555]

Cheng IH, Scearce-Levie K, Legleiter J, Palop JJ, Gerstein H, Bien-Ly N, Puolivali J, Lesne S, Ashe KH, Muchowski PJ, et al. Accelerating amyloid-beta fibrillization reduces oligomer levels and functional deficits in Alzheimer disease mouse models. J Biol Chem 2007;282:23818–23828. [PubMed: 17548355]

Clelland CD, Choi M, Romberg C, Clemenson GD Jr, Fragniere A, Tyers P, Jessberger S, Saksida LM, Barker RA, Gage FH, et al. A functional role for adult hippocampal neurogenesis in spatial pattern separation. Science 2009;325:210–213. [PubMed: 19590004]

Dineley KT, Hogan D, Zhang WR, Taglialatela G. Acute inhibition of calcineurin restores associative learning and memory in Tg2576 APP transgenic mice. Neurobiol Learn Mem 2007;88:217–224. [PubMed: 17521929]

Donovan MH, Yazdani U, Norris RD, Games D, German DC, Eisch AJ. Decreased adult hippocampal neurogenesis in the PDAPP mouse model of Alzheimer's disease. J Comp Neurol 2006;495:70–83. [PubMed: 16432899]

Duan X, Chang JH, Ge S, Faulkner RL, Kim JY, Kitabatake Y, Liu XB, Yang CH, Jordan JD, Ma DK, et al. Disrupted-In-Schizophrenia 1 regulates integration of newly generated neurons in the adult brain. Cell 2007;130:1146–1158. [PubMed: 17825401]

Eriksson PS, Perfilieva E, Bjork-Eriksson T, Alborn AM, Nordborg C, Peterson DA, Gage FH. Neurogenesis in the adult human hippocampus. Nat Med 1998;4:1313–1317. [PubMed: 9809557]

Fernandez F, Morishita W, Zuniga E, Nguyen J, Blank M, Malenka RC, Garner CC. Pharmacotherapy for cognitive impairment in a mouse model of Down syndrome. Nat Neurosci 2007;10:411–413. [PubMed: 17322876]

Freund TF, Buzsaki G. Interneurons of the hippocampus. Hippocampus 1996;6:347–470. [PubMed: 8915675]

Gan L, Qiao S, Lan X, Chi L, Luo C, Lien L, Yan Liu Q, Liu R. Neurogenic responses to amyloid-beta plaques in the brain of Alzheimer's disease-like transgenic (pPDGF-APPSw,Ind) mice. Neurobiol Dis 2008;29:71–80. [PubMed: 17916429]

Ganguly K, Schinder AF, Wong ST, Poo M. GABA itself promotes the developmental switch of neuronal GABAergic responses from excitation to inhibition. Cell 2001;105:521–532. [PubMed: 11371348]

Ge S, Goh EL, Sailor KA, Kitabatake Y, Ming GL, Song H. GABA regulates synaptic integration of newly generated neurons in the adult brain. Nature 2006;439:589–593. [PubMed: 16341203]

Ge S, Sailor KA, Ming GL, Song H. Synaptic integration and plasticity of new neurons in the adult hippocampus. J Physiol 2008;586:3759–3765. [PubMed: 18499723]

Ge S, Yang CH, Hsu KS, Ming GL, Song H. A critical period for enhanced synaptic plasticity in newly generated neurons of the adult brain. Neuron 2007;54:559–566. [PubMed: 17521569]

Haughey NJ, Nath A, Chan SL, Borchard AC, Rao MS, Mattson MP. Disruption of neurogenesis by amyloid beta-peptide, and perturbed neural progenitor cell homeostasis, in models of Alzheimer's disease. J Neurochem 2002;83:1509–1524. [PubMed: 12472904]

Hsieh H, Boehm J, Sato C, Iwatsubo T, Tomita T, Sisodia S, Malinow R. AMPAR removal underlies Abeta-induced synaptic depression and dendritic spine loss. Neuron 2006;52:831–843. [PubMed: 17145504]

Imayoshi I, Sakamoto M, Ohtsuka T, Takao K, Miyakawa T, Yamaguchi M, Mori K, Ikeda T, Itohara S, Kageyama R. Roles of continuous neurogenesis in the structural and functional integrity of the adult forebrain. Nat Neurosci 2008;11:1153–1161. [PubMed: 18758458]

Jin K, Galvan V, Xie L, Mao XO, Gorostiza OF, Bredesen DE, Greenberg DA. Enhanced neurogenesis in Alzheimer's disease transgenic (PDGF-APPSw, Ind) mice. Proc Natl Acad Sci U S A 2004a; 101:13363–13367. [PubMed: 15340159]

Jin K, Peel AL, Mao XO, Xie L, Cottrell BA, Henshall DC, Greenberg DA. Increased hippocampal neurogenesis in Alzheimer's disease. Proc Natl Acad Sci USA 2004b;101:343–347. [PubMed: 14660786]

Johnson-Wood K, Lee M, Motter R, Hu K, Gordon G, Barbour R, Khan K, Gordon M, Tan H, Games D, et al. Amyloid precursor protein processing and Aβ42 deposition in a transgenic mouse model of Alzheimer disease. Proc Natl Acad Sci USA 1997;94:1550–1555. [PubMed: 9037091]

Li B, Yamamori H, Tatebayashi Y, Shafit-Zagardo B, Tanimukai H, Chen S, Iqbal K, Grundke-Iqbal I. Failure of neuronal maturation in Alzheimer disease dentate gyrus. J Neuropathol Exp Neurol 2008;67:78–84. [PubMed: 18091557]

Lopez-Toledano MA, Shelanski ML. Increased neurogenesis in young transgenic mice overexpressing human APP(Sw, Ind). J Alzheimers Dis 2007;12:229–240. [PubMed: 18057556]

McGowan E, Pickford F, Kim J, Onstead L, Eriksen J, Yu C, Skipper L, Murphy MP, Beard J, Das P, et al. Abeta42 is essential for parenchymal and vascular amyloid deposition in mice. Neuron 2005;47:191–199. [PubMed: 16039562]

Moolman DL, Vitolo OV, Vonsattel JP, Shelanski ML. Dendrite and dendritic spine alterations in Alzheimer models. J Neurocytol 2004;33:377–387. [PubMed: 15475691]

Mucke L, Masliah E, Yu G-Q, Mallory M, Rockenstein EM, Tatsuno G, Hu K, Kholodenko D, Johnson-Wood K, McConlogue L. High-level neuronal expression of $A\beta_{1–42}$ in wild-type human amyloid

protein precursor transgenic mice: Synaptotoxicity without plaque formation. J Neurosci 2000;20:4050–4058. [PubMed: 10818140]

Mueller-Steiner S, Zhou Y, Arai H, Roberson ED, Sun B, Chen J, Wang X, Yu G, Esposito L, Mucke L, et al. Antiamyloidogenic and neuroprotective functions of cathepsin B: implications for Alzheimer's disease. Neuron 2006;51:703–714. [PubMed: 16982417]

Owens DF, Kriegstein AR. Is there more to GABA than synaptic inhibition? Nat Rev Neurosci 2002;3:715–727. [PubMed: 12209120]

Palop JJ, Chin J, Roberson ED, Wang J, Thwin MT, Bien-Ly N, Yoo J, Ho KO, Yu GQ, Kreitzer A, et al. Aberrant excitatory neuronal activity and compensatory remodeling of inhibitory hippocampal circuits in mouse models of Alzheimer's disease. Neuron 2007;55:697–711. [PubMed: 17785178]

Paxinos, G.; Franklin, KJ. The Mouse Brain in Stereotaxic Coordinates. Second edn. Academic Press; 2001.

Santarelli L, Saxe M, Gross C, Surget A, Battaglia F, Dulawa S, Weisstaub N, Lee J, Duman R, Arancio O, et al. Requirement of hippocampal neurogenesis for the behavioral effects of antidepressants. Science 2003;301:805–809. [PubMed: 12907793]

Saxe MD, Battaglia F, Wang JW, Malleret G, David DJ, Monckton JE, Garcia AD, Sofroniew MV, Kandel ER, Santarelli L, et al. Ablation of hippocampal neurogenesis impairs contextual fear conditioning and synaptic plasticity in the dentate gyrus. Proc Natl Acad Sci U S A 2006;103:17501–17506. [PubMed: 17088541]

Scheff SW, Price DA. Synaptic pathology in Alzheimer's disease: a review of ultrastructural studies. Neurobiol Aging 2003;24:1029–1046. [PubMed: 14643375]

Schmidt-Hieber C, Jonas P, Bischofberger J. Enhanced synaptic plasticity in newly generated granule cells of the adult hippocampus. Nature 2004;429:184–187. [PubMed: 15107864]

Shankar GM, Bloodgood BL, Townsend M, Walsh DM, Selkoe DJ, Sabatini BL. Natural oligomers of the Alzheimer amyloid-beta protein induce reversible synapse loss by modulating an NMDA-type glutamate receptor-dependent signaling pathway. J Neurosci 2007;27:2866–2875. [PubMed: 17360908]

Shankar GM, Li S, Mehta TH, Garcia-Munoz A, Shepardson NE, Smith I, Brett FM, Farrell MA, Rowan MJ, Lemere CA, et al. Amyloid-beta protein dimers isolated directly from Alzheimer's brains impair synaptic plasticity and memory. Nat Med. 2008

Shors TJ, Miesegaes G, Beylin A, Zhao M, Rydel T, Gould E. Neurogenesis in the adult is involved in the formation of trace memories. Nature 2001;410:372–376. [PubMed: 11268214]

Snyder EM, Nong Y, Almeida CG, Paul S, Moran T, Choi EY, Nairn AC, Salter MW, Lombroso PJ, Gouras GK, et al. Regulation of NMDA receptor trafficking by amyloid-beta. Nat Neurosci 2005a; 8:1051–1058. [PubMed: 16025111]

Snyder JS, Hong NS, McDonald RJ, Wojtowicz JM. A role for adult neurogenesis in spatial long-term memory. Neuroscience 2005b;130:843–852. [PubMed: 15652983]

Taglialatela G, Hogan D, Zhang WR, Dineley KT. Intermediate- and long-term recognition memory deficits in Tg2576 mice are reversed with acute calcineurin inhibition. Behav Brain Res 2009;200:95–99. [PubMed: 19162087]

Tanzi RE, Bertram L. Twenty years of the Alzheimer's disease amyloid hypothesis: a genetic perspective. Cell 2005;120:545–555. [PubMed: 15734686]

Tashiro A, Sandler VM, Toni N, Zhao C, Gage FH. NMDA-receptor-mediated, cell-specific integration of new neurons in adult dentate gyrus. Nature 2006a;442:929–933. [PubMed: 16906136]

Tashiro A, Zhao C, Gage FH. Retrovirus-mediated single-cell gene knockout technique in adult newborn neurons in vivo. Nat Protoc 2006b;1:3049–3055. [PubMed: 17406567]

Tozuka Y, Fukuda S, Namba T, Seki T, Hisatsune T. GABAergic excitation promotes neuronal differentiation in adult hippocampal progenitor cells. Neuron 2005;47:803–815. [PubMed: 16157276]

van Praag H, Schinder AF, Christie BR, Toni N, Palmer TD, Gage FH. Functional neurogenesis in the adult hippocampus. Nature 2002;415:1030–1034. [PubMed: 11875571]

Verret L, Trouche S, Zerwas M, Rampon C. Hippocampal neurogenesis during normal and pathological aging. Psychoneuroendocrinology 2007;32 Suppl 1:S26–S30. [PubMed: 17629417]

Yoshiike Y, Kimura T, Yamashita S, Furudate H, Mizoroki T, Murayama M, Takashima A. GABA(A) receptor-mediated acceleration of aging-associated memory decline in APP/PS1 mice and its pharmacological treatment by picrotoxin. PLoS One 2008;3:e3029. [PubMed: 18716656]

Zhao C, Deng W, Gage FH. Mechanisms and functional implications of adult neurogenesis. Cell 2008;132:645–660. [PubMed: 18295581]

Zhao C, Teng EM, Summers RG Jr, Ming GL, Gage FH. Distinct morphological stages of dentate granule neuron maturation in the adult mouse hippocampus. J Neurosci 2006;26:3–11. [PubMed: 16399667]

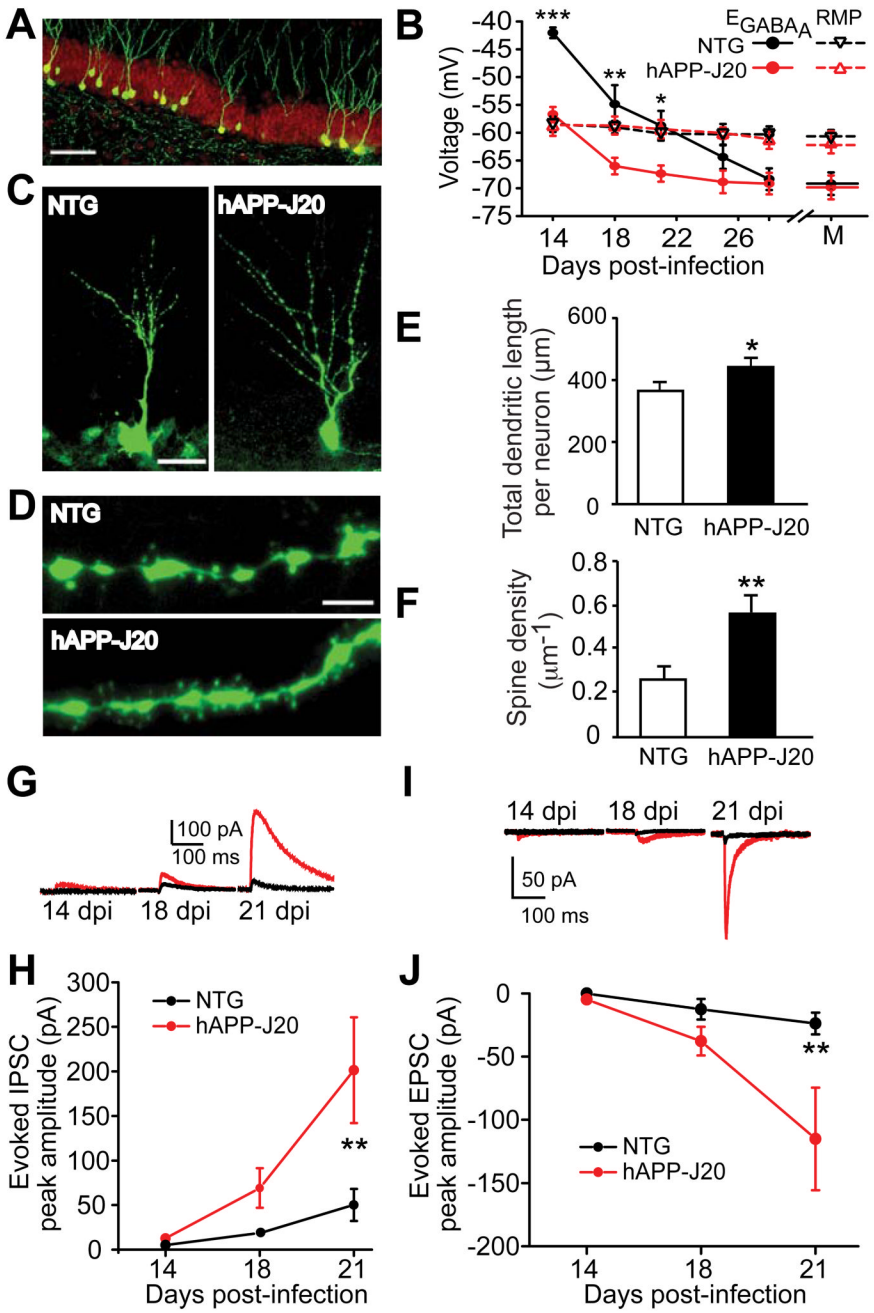

Figure 1. Accelerated Early Morphological and Functional Development of Adult-Born GCs in 2–3-Month-Old hAPP-J20 Mice

(A) Photomicrograph of 28-day-old adult-born GCs labeled by CAG-EGFP retrovirus (green) and stained with an anti-NeuN antibody (red).

(B) $GABA_A$ Cl^- current reversal potentials (E_{GABA}) and resting membrane potentials (RMP) of adult-born GCs at 14-, 18-, 21-, 25-, or 28-dpi and of mature (M) GCs in hAPP-J20 and NTG mice. n = 6–7 neurons obtained from 3–4 mice per genotype and dpi. For E_{GABA}, genotype $F_{(1, 63)} = 31.87$; *, $P < 0.05$; **, $P < 0.01$; ***, $P < 0.001$; by two-way ANOVA and Bonferonni posthoc test.

(C, D) Photomicrographs of 18-day-old adult-born GCs (C) and their dendritic spines (D) in hAPP-J20 and NTG mice.

(E, F) Quantification of total dendritic length (E) and dendritic spine density (F) of adult-born GCs at 18 dpi in hAPP-J20 and NTG mice. n = 41–44 neurons (for dendritic length) and n = 17–30 dendritic segments (for spine density) from 5 mice per genotype. *, $P < 0.05$; **, $P < 0.01$, unpaired student's t test.

(G, I) Representative traces of evoked inhibitory postsynaptic currents (eIPSCs) (G) or evoked excitatory postsynaptic currents (eEPSCs) (I) of 14-, 18-, and 21-day-old adult-born GCs in hAPP-J20 (red) and NTG (black) mice.

(H, J) Quantifications of peak amplitudes of eIPSCs (H) and eEPSCs (J) of 14-, 18-, or 21-day-old adult-born GCs in hAPP-J20 (red) and NTG mice (black). H: n = 5–11 neurons from 2–3 mice per genotype and dpi, genotype $F_{(1,50)} = 1.194$; **, $P < 0.01$. J: n = 5 –10 neurons from 2–3 mice per genotype and per dpi, genotype $F_{(1,51)} = 23.68$; **, $P < 0.01$; by two-way ANOVA, Bonferroni posthoc test.

Values are means ± SEM (E, F). Scale bars: 50 μm (A), 20 μm (C), 3 μm (D).

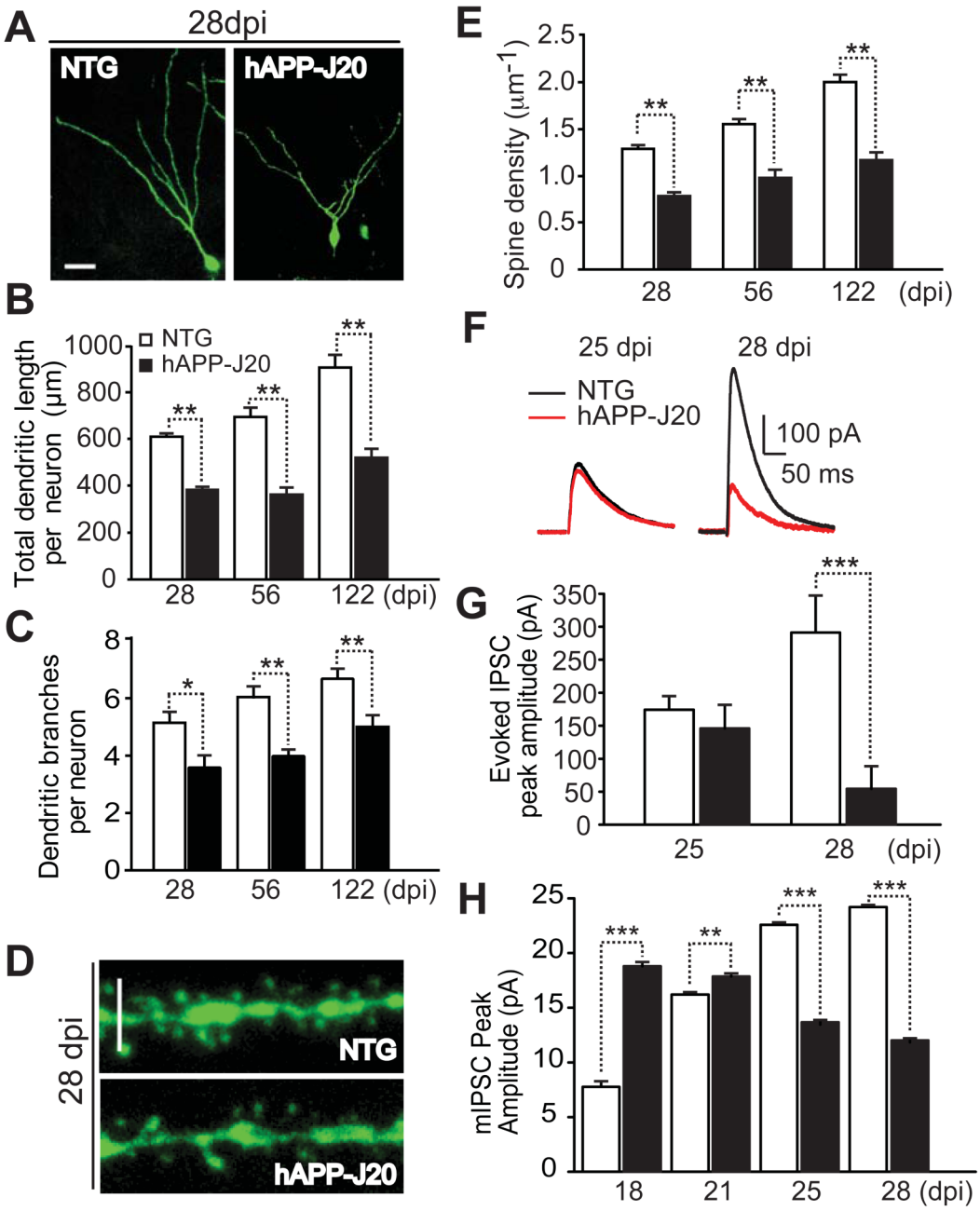

Figure 2. Impaired Maturation and Function of Adult-Born GCs in 2–3-Month-Old hAPP-J20 Mice

(A) Photomicrographs of 28-day-old adult-born GCs in hAPP-J20 and NTG mice.

(B, C) Quantification of dendritic length (B) and branches (C) of 28-, 56- and 122-day-old adult-born GCs in hAPP-J20 and NTG mice. At 28 dpi, n = 84–94 neurons from 11– 16 mice per genotype; at 56 dpi, n = 19–30 neurons from 3 mice per genotype; at 122 dpi, n = 16–19 neurons from 3 mice per genotype. *, $P < 0.05$; **, $P < 0.01$, unpaired student's t test.

(D) Photomicrographs of dendritic segments from 28-day-old adult-born GCs in hAPP-J20 and NTG mice.

(E) Quantification of spine density of 28-, 56- and 122-day-old adult-born GCs in hAPP-J20 and NTG mice. At 28 dpi, n = 91–100 dendritic segments from 11–12 mice per genotype; At 56 dpi, n = 21–31 segments from 3 mice; At 122 dpi, n = 18–20 segments from 3 mice per genotype. **, $P < 0.01$, unpaired student's t test.
(F, G) Representative traces (F) and quantification (G) of eIPSC of adult-born GCs at 25-and 28 dpi in hAPP-J20 and NTG mice. n = 5–8 neurons from 3–4 mice per genotype and dpi, genotype $F_{(1,50)} = 1.194$; ***, $P < 0.001$ by two-way ANOVA, Bonferroni posthoc test.
(H) Quantification of the peak amplitudes of mIPSCs of 18-, 21-, 25-, and 28-dpi adult-born GCs in hAPP-J20 and NTG mice. n = 5–8 neurons from 3–4 mice per genotype, genotype $F_{(1,42)} = 100.0$; **, $P < 0.01$; ***, $P < 0.001$ by two-way ANOVA, Bonferroni posthoc test. Statistics performed on all data from 18- to 28- dpi (G and H).
Values are means ± SEM (B, C, E, G, H). Scale bars: 20 μm (A), 3 μm (D).

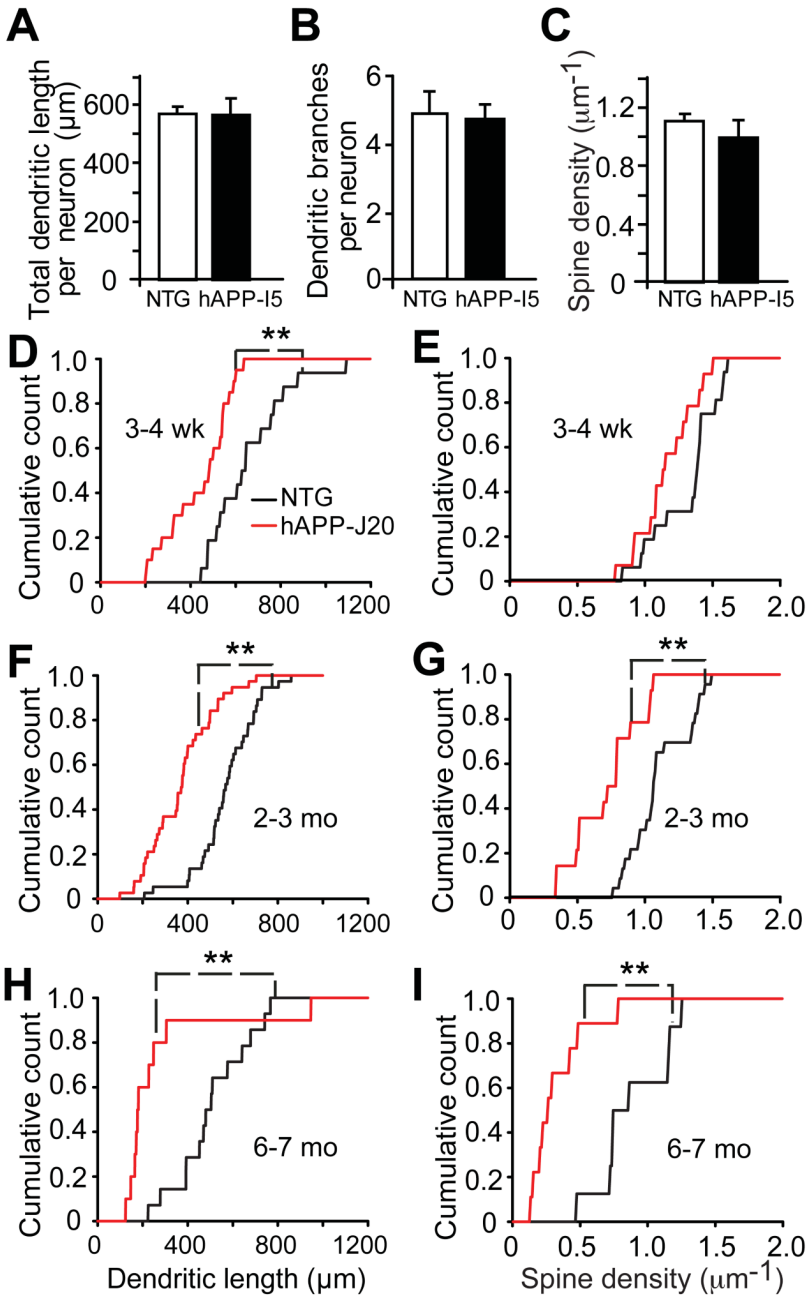

Figure 3. Dendritic Maturation of Newborn GCs Is Affected by Age but Not by Wildtype hAPP

(A–C) The 28-day-old adult-born GCs in 2–3-month-old hAPP-I5 and NTG mice had similar total denedritic lengths (A), number of denedritic branching points (B), and spine densities (C). Values are means ± SEM.

(D–I) Cumulative counts of the total dendritic length (D, F, H) and spine density (E, G, I) of 28-day-old newborn GCs in 3–4-week-old (D, E), 2–3-month-old (F, G) and 6–7-month-old (H, I) hAPP-J20 (red) and NTG (black) mice. n = 10–20 neurons from 3–4 mice per genotype. Two-sample Kolmogorov-Smirnov test revealed genotype differences (**, $P < 0.01$) in (D, F, G, H, and I), but not in (E). wk: weeks; mo: months.

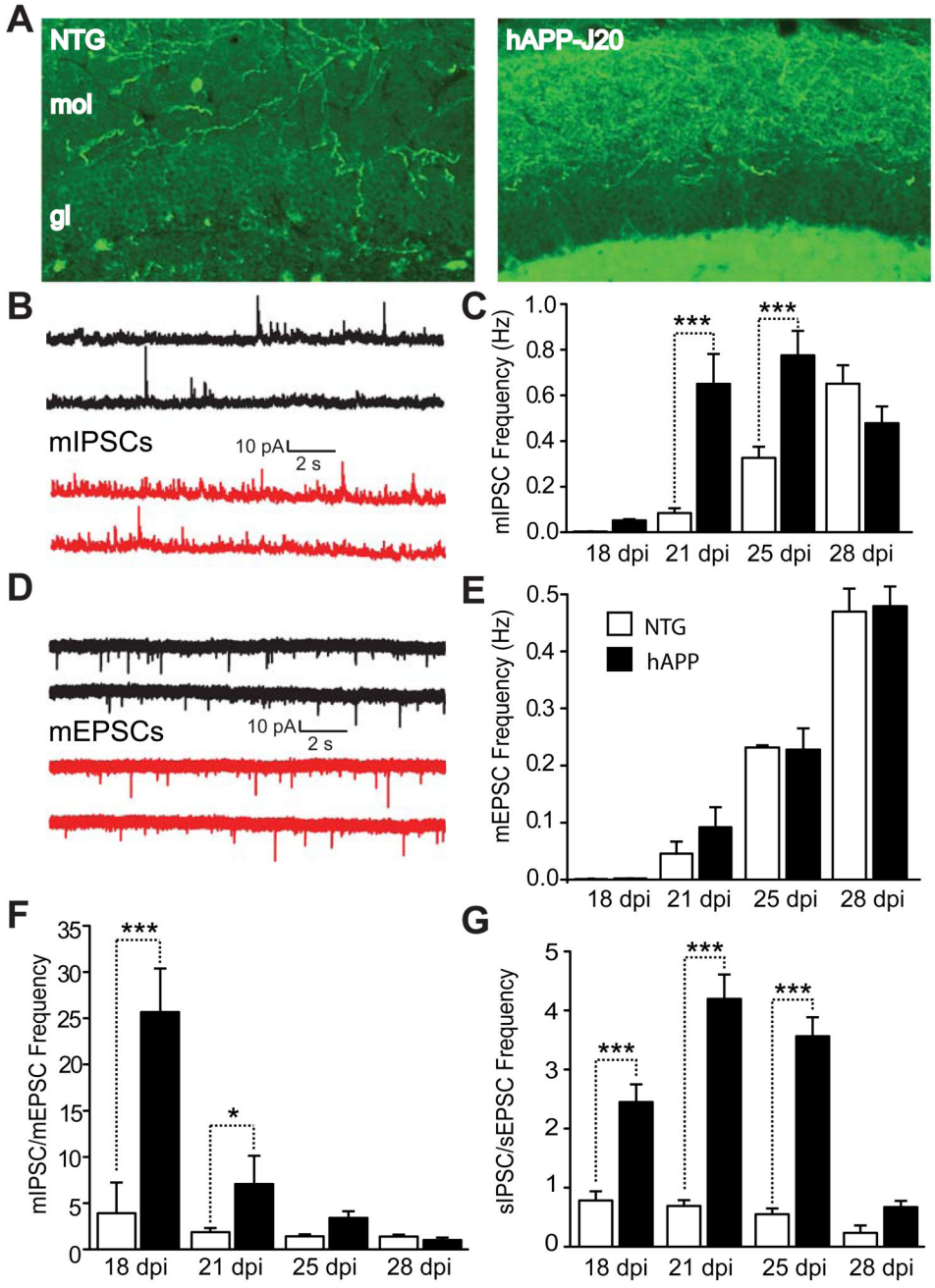

Figure 4. Excessive GABAergic Inputs onto Adult-Born GCs in 2–3-month-old hAPP-J20 Mice

(A) Brain sections stained with an antibody against NPY. Compared with NTG mice (left), hAPP-J20 mice (right) showed increased NPY/GABAergic sprouting in the molecular layer. mol, molecular layer; gl, granular layer.

(B, D) Representative traces of mIPSCs (B) and mEPSCs (D) of 21-day-old adult-born GCs in 2–3-month-old NTG (black) and hAPP-J20 (red) mice.

(C, E) Quantification of mIPSC frequency (C) and mEPSC frequency (E) of adult-born GCs in hAPP-J20 and NTG mice at 18-, 21-, 25- and 28-dpi. n = 7–12 neurons from 3 mice per genotype and dpi. C: genotype $F_{(1,47)} = 17.47$; E: genotype $F_{(1,37)} = 0.5096$; ***, $P < 0.001$, two-way ANOVA, Bonferroni posthoc test.

(F, G) Ratios of mIPSC/mEPSC frequency (F) or sIPSC/sEPSC frequency (G) in adult-born GCs in hAPP-J20 and NTG mice at 18-, 21-, 25- or 28-dpi. F: n = 7–12 neurons from 3 mice per genotype and dpi, genotype $F_{(1,37)} = 28.02$. G: n = 6–7 neurons, 3 mice per genotype and dpi, genotype $F_{(1,41)} = 173.0$. *, $P < 0.05$; ***, $P < 0.001$, two-way ANOVA, Bonferroni posthoc test. Values are means ± SEM (C, E–G).

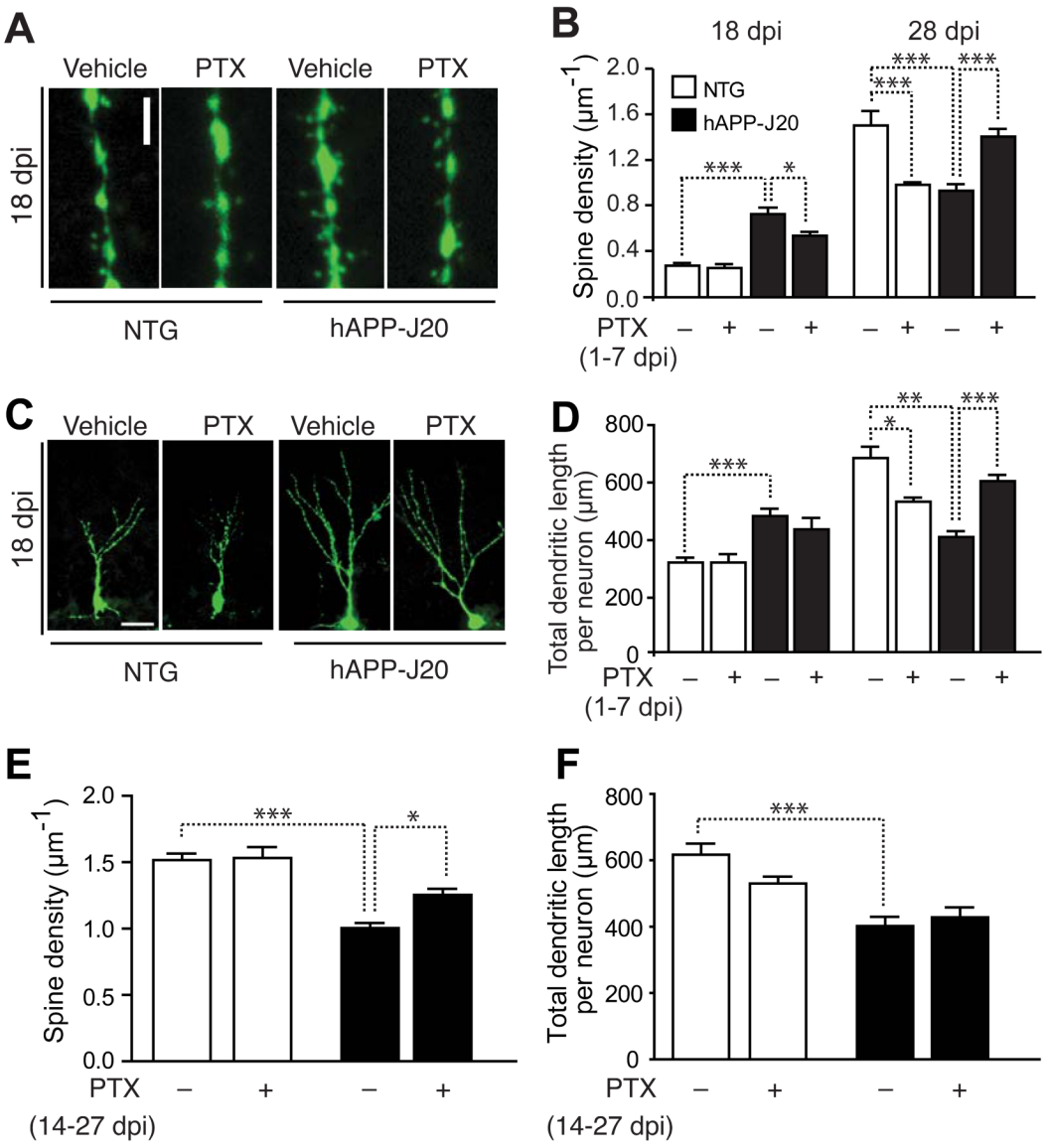

Figure 5. Treatment with $GABA_A$ Receptor Antagonist PTX Ameliorates Developmental Alterations of Adult-Born GCs in 2–3-Month-Old hAPP-J20 Mice

(A, C) Photomicrographs of spines (A) and dendrites (C) of 18-day-old adult-born GCs in hAPP-J20 and NTG mice treated with vehicle or PTX (1.0 mg/kg body weight) from 1–7 dpi. Scale bars: 3 μm (A), 20 μm (C).

(B, D) Quantification of spine densities (B) and dendritic lengths (D) in 18- and 28-day-old adult-born GCs of hAPP and NTG mice treated with vehicle or PTX from 1–7 dpi. A two-way ANOVA analysis revealed significant genotype effects on spine density (B) at 18 dpi ($F_{(1,96)} = 70.21$, $P < 0.0001$) and 28 dpi ($F_{(1,184)} = 7.067$, $P = 0.0085$), on dendritic length (D) at 18 dpi ($F_{(1,184)} = 42.07$, $P < 0.0001$) and 28 dpi ($F_{(1,134)} = 9.360$, $P = 0.0027$), significant PTX effects on spine density (B) at 18 dpi (B: $F_{(1,96)} = 5.673$, $P = 0.0192$), and significant genotype × PTX interactions for both spine density (B) ($F_{(1,184)} = 49.52$, $P < 27\ 0.0001$) and dendritic length (D) ($F_{(1,134)} = 22.05$, $P < 0.0001$) at 28 dpi. *, $P < 0.05$; **, $P < 0.01$; ***, $P < 0.001$, Bonferroni posthoc test.

(E, F) Quantification of spine densities (E) and dendritic lengths (F) in 28-day-old adult-born GCs of hAPP-J20 and NTG mice treated with vehicle or PTX from 14–27 dpi. A two-way ANOVA identified a significant main effect of genotype for both spine density (E: $F_{(1,151)}$ = 52.79, $P < 0.0001$) and dendritic length (F: $F_{(1,138)} = 32.72$, $P < 0.0001$), a significant PTX effects on spine density (E: $F_{(1,151)} = 6.038$, $P = 0.0151$), and a significant genotype × PTX interaction for both spine density (E: $F_{(1,151)} = 4.550$, $P = 0.0345$) and dendritic length (F: $F_{(1,138)} = 4.173$, $P = 0.0430$). *, $P < 0.05$; ***, $P < 0.001$, Bonferroni posthoc test. Values are means ± SEM (B, D–F).

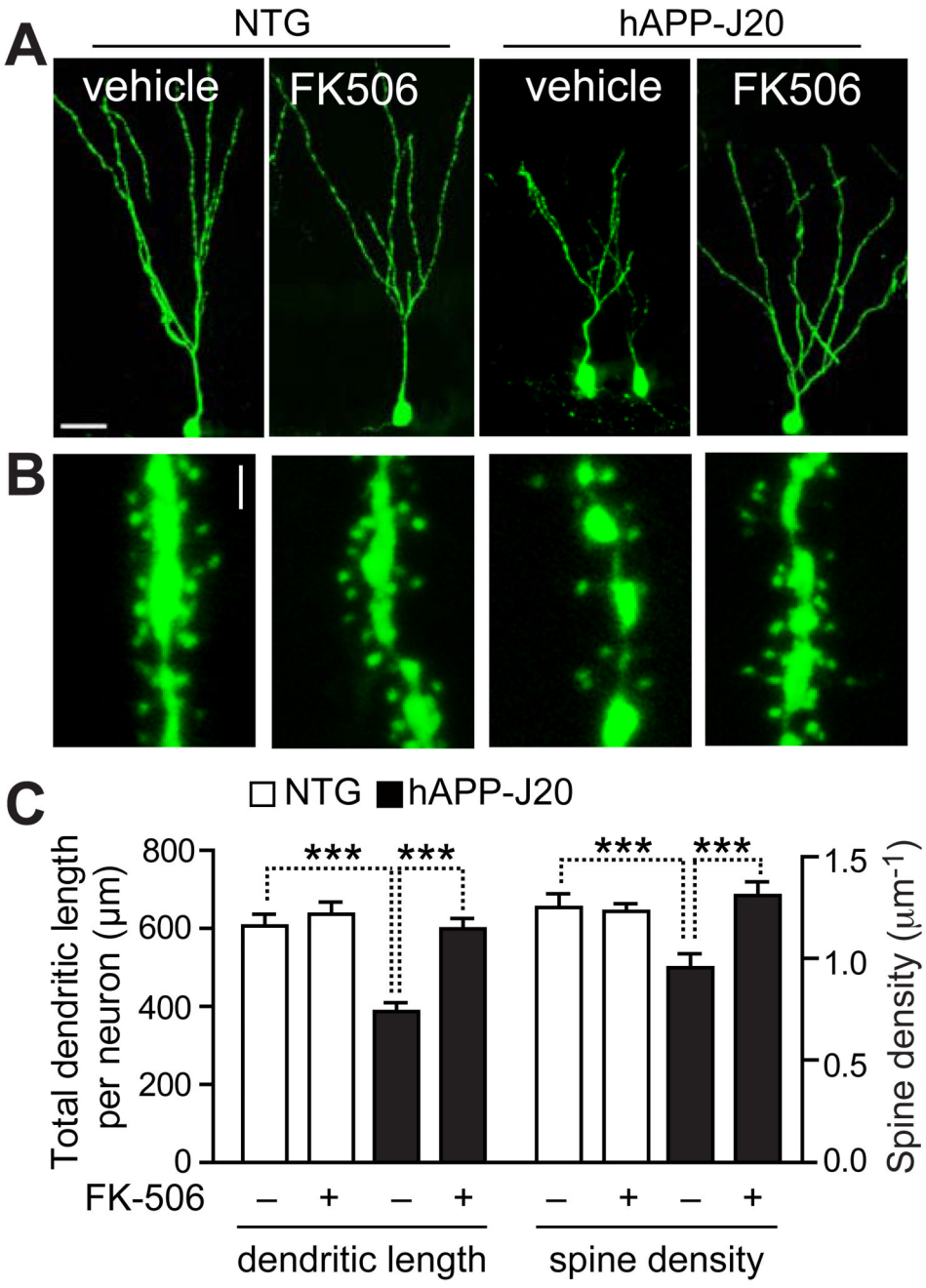

Figure 6. Effect of FK506 on Dendritic Maturation of Adult-Born GCs

(A, B) Photomicrographs of dendrites (A) and spines (B) of 28-day-old adult-born GCs in 2–3-month-old NTG and hAPP-J20 mice treated with vehicle or FK506 (5 mg/kg) from 14–27 dpi. Scale bars: 20 μm (A), or 3 μm (B).

(C) Quantification of dendritic length and spine density of 28-day-old adult-born GCs in 2–3-month-old NTG and hAPP-J20 mice treated with vehicle or with 5 mg/kg of FK506. A two-way ANOVA analysis identified a significant genotype effect on both dendritic length ($F_{(1,167)} = 19.22$, $P < 0.0001$) and spine density ($F_{(1,104)} = 4.338$, $P = 0.0397$), a significant main effect of FK506 treatment on both dendritic length ($F_{(1,167)} = 17.08$, $P < 0.0001$) and spine density ($F_{(1,104)} = 6.033$, $P = 0.0157$), and a significant genotype × FK506 treatment

interaction for both dendritic length ($F_{(1,167)} = 9.664$, $P = 0.0022$) and spine density ($F_{(1,104)} = 11.27$, $P = 0.0011$). ***, $P < 0.001$, Bonferroni posthoc test. Values are means ± SEM.